1997

# Radio emission from objects in the Hubble deep field

E. B. Fomalont

K. I. Kellermann

Eric A. Richards

Bruce Partridge
*Haverford College*, bpartrid@haverford.edu



Repository Citation
(with E. B. Fomalont et al.) Radio Emission from Objects in the Hubble Deep Field, Ap. J. (Letters), 475, L5, 1997.

1997

# Radio emission from objects in the Hubble deep field

Edward B. Fomalont

K. I. Kellermann

Eric A. Richards

R. Bruce Partridge
*Haverford College*



Repository Citation
(with E. B. Fomalont et al.) Radio Emission from Objects in the Hubble Deep Field, Ap. J. (Letters), 475, L5, 1997.

The Astrophysical Journal, 475:L5–L7, 1997 January 20


# RADIO EMISSION FROM OBJECTS IN THE HUBBLE DEEP FIELD

E. B. Fomalont and K. I. Kellermann
National Radio Astronomy Observatory
E. A. Richards
University of Virginia and National Radio Astronomy Observatory
R. A. Windhorst
Arizona State University
and
R. B. Partridge
Haverford College
*Received 1996 August 5; accepted 1996 October 31*

## ABSTRACT

A radio image that covers the Hubble deep field and flanking fields has been made using the VLA for 50 hr at a frequency of 8.4 GHz, a resolution of 6″, and a 4.3 $\sigma$ detection level of 12.2 $\mu$Jy. All six radio sources detected in the deep field are identified with galaxies brighter than $I$ = 24 mag, based on a radio/optical coincidence better than 1″. In the flanking fields 8 of 12 sources are identified with galaxies 19 to 25 mag. The identifications are preferentially with red elliptical galaxies and early-type spiral galaxies. Several galaxies show distortions that suggest interaction.

*Subject headings:* galaxies: active — radio continuum: galaxies

## 1. INTRODUCTION

The Hubble deep field (HDF) project was commissioned in order to utilize the superior imaging capabilities of the *Hubble Space Telescope* to study galaxy populations at cosmological distances. The field is centered near $\alpha = 12^h36^m49^s$, $\delta = +62°12'58''$ (epoch J2000) and covers a region of about 4 arcmin$^2$. Galaxies as faint as 29 mag can be detected. Shallower observations, of eight additional WFPC2 fields surrounding the HDF (Hubble flanking fields [HFF]), were added to cover an area of about 40 arcmin$^2$ with a detection level of 25 mag (Williams et al. 1996). Intense study at all wavelengths of this region of sky is in progress at many observatories.

The radio emission from objects in the HDF and the surrounding flanking fields is important in understanding the space density and evolution of radio sources, since virtually all of the objects should be identified (see, e.g., Windhorst, Dressler, & Koo 1987). Recent observations of faint microjansky radio galaxies (Windhorst et al. 1993, 1995; Kellermann et al. 1996) show that these weaker sources do not comprise as homogeneous a population of starburst spiral galaxies as do the millijansky sources. Many of these microjansky radio sources have been optically identified with field spirals as well as red ellipticals. Less than 10% of the identifications are with quasars or stars. Many of these radio sources are concentrated in small groups and are morphologically peculiar, indicating that tidal interactions may play an important role in galaxy evolution and its associated microwave emission at this epoch (Fomalont et al. 1991; Windhorst et al. 1995; Hammer et al. 1995).

This paper reports on the initial results from the first deep radio observations of the HDF and HFF. Fourteen of the 18 radio sources have been identified with optical objects, and another three of the remaining four sources have possible identifications with nearby objects.

## 2. THE HDF RADIO IMAGE

Observations to image the HDF were made with the VLA in the C configuration between 1996 February 5 and March 12 on six separate days; each run was 10 hr in length. The field center for the radio observations was $\alpha = 12^h36^m49\overset{s}{.}4$, $\delta = +62°12'58''$ (epoch J2000). The full width at half-power (FWHM) of the VLA is 312″, and radio sources were detected in a field of view of diameter 480″. Observations were alternated between the HDF and the calibrator source 1217+585, 13 minutes on HDF and 2 minutes on 1217+585. The assumed position of 1217+585 is $\alpha = 12^h17^m11\overset{s}{.}203$, $\delta = +58°35'26\overset{''}{.}228$ (epoch J2000) and is accurate to $0\overset{''}{.}02$. The source 3C 286 was observed once each day in order to determine the flux density scale of the system. The editing, calibration, imaging, and cleaning of the data were made in the normal manner using the Astronomical Image Processing System, and the details are described in Fomalont et al. (1993).

The clean image that covers the HDF and HFF is shown in Figure 1. The rms noise is 2.78 $\mu$Jy at the image center. Sources with a peak image flux density greater than 12.2 $\mu$Jy (4.3 $\sigma$) have a greater than 95% probability of being real sources in the sky. Figure 1 is uncorrected for the primary-beam attenuation, and the middle of the HDF lies to the right of the center of the image. There are 18 radio sources above 12.2 $\mu$Jy.

Tables 1 and 2 list the parameters for the six radio sources found in the HDF and the 12 sources in the HFF, respectively. The sources are listed by increasing right ascension order. Source names are derived from the minutes and seconds of the source coordinates. The integrated image flux density and sky flux density, corrected for the primary-beam attenuation, are

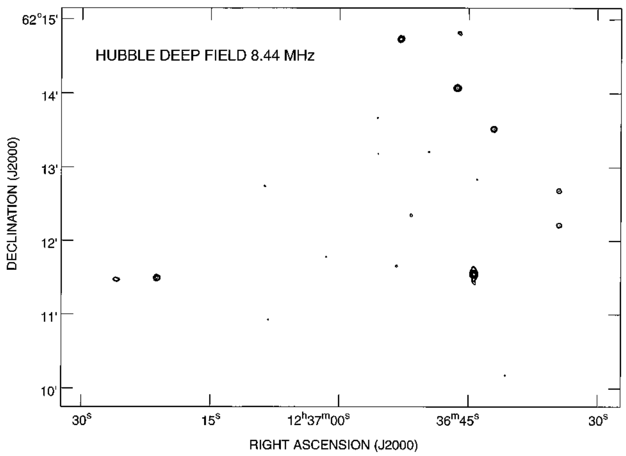


FIG. 1.—Radio emission from the HDF and the HFF. The contour levels are at 12.3, 18, 36, 72, 144, and 288 $\mu$Jy beam$^{-1}$, and 18 sources have been detected. The resolution is 6″, which gives the best signal-to-noise ratio. No correction has been made for the primary-beam sensitivity of the VLA telescopes.

given (with error estimates) in the next two columns. For sources outside of the 8% power level of the primary beam, the true sky flux density cannot be accurately determined. The next two columns give the right ascension and the declination (with errors) of the centroid of each source. These are followed by the angular size estimate or limit (14 of the 18 sources are unresolved), and then the redshift (Cohen et al. 1996). For both tables we list our estimate of the $I$-magnitude of the identification, as measured from the HDF or the HFF images. A question mark indicates a possible identification with an object which is less than 2″ away from the radio position. The source HFF 3646+1448 in one of the flanking fields appears to be in an empty field.

The radio positions given in Tables 1 and 2 are tied to the inertial quasar reference frame (by using the quasar 1217+585 as the primary position calibrator) to an accuracy better than 0″.02; however, the noise in the images limits the positional accuracy of most sources to 0″.3 in each coordinate. These sources can be used to determine the most accurate registration of the HDF using the best identification, and further radio observations at higher resolution should produce an alignment of the radio and optical grids to better than 0″.1.

## 3. THE OPTICAL IDENTIFICATIONS

The optical identification of the weak radio sources with faint galaxies requires an alignment of the radio and optical grids to better than 1″. However, the guide star positions used by *Hubble* to determine its a priori registration can be up to 2″ in error, and these can produce offsets in each of the HDF+HFF frames from the radio FK5 frame by over 1″. A more accurate HDF+HFF registration with respect to the FK5 frame is currently being made by a comparison with an astrometric quality Palomar image provided by C. Steidel and by using these high-quality identifications of radio sources. For the HDF image, we estimate that the a priori positional accuracy is better than 0″.5; for some of the HFF images the position error may be larger than 1″.

Nevertheless, most radio sources can be unambiguously identified even with the present astrometric precision. Figures 2*a* and 2*b* (Plates L3, L4) show the radio/optical fields for each of the 18 sources. Each square box covers an area of 20″ × 20″, centered on the radio source. The gray scale shows the optical emission (the gray scale is different for the HDF and the HFF) with the optical resolution convolved to 0″.2. The radio emission contour levels are 6, 12, 18, and 36 $\mu$Jy beam$^{-1}$, and are uncorrected for the primary-beam attenuation. Only radio sources with a central peak above the second contour level should be considered real sources. However, there are some interesting tentative identifications with weaker radio objects in some of the fields; deeper radio observations now underway will produce further firm identifications. The nature and reliability of the identification of each source are given in the individual figure captions and are discussed further below.

1. The source HDF 3649+1313 is near the center of the *Hubble* field where the radio sensitivity is at maximum. The peak emission is identified with a distorted galaxy, and emission extends to the north and west to other distorted galaxies in this probable interacting system.
2. Source HDF 3644+1133 is intriguing. It is one of the brightest sources in the radio field and is identified with a typical red elliptical galaxy. This main radio component is less than 2″ in diameter, but there is also low-level radio emission extending north and south from the peak. The northern spur ends near a peculiar-looking blue chain galaxy; the southern spur curves west to a small asymmetric object (on the flanking field). Higher resolution radio observations are needed to determine whether the emission peaks are connected or merely blended together in this relatively low-resolution radio image.
3. Source HFF 3634+1212 appears to be an interacting system; source HFF 3701+1147 lies at the end of an arc that eminates from the nearby 22 mag galaxy (this feature is weak on the HFF and must be confirmed); one source

TABLE 1
RADIO SOURCES IN THE HUBBLE DEEP FIELD

| Name | Flux Density ($\mu$Jy) Image | Flux Density ($\mu$Jy) Sky | Right Ascension[a] (J2000) | Declination[a] (J2000) | Size (arcsec) | $z$ | $I$ |
|---|---|---|---|---|---|---|---|
| 3644+1249 | 13 ± 3 | 15 ± 3 | 12 36 44.02 ± 0.07 | 62 12 49.9 ± 0.6 | <2 | 0.556 | 21 |
| 3644+1133 | 458 ± 3 | 783 ± 5 | 12 36 44.38 ± 0.02 | 62 11 33.0 ± 0.2 | <2 | 1.013 | 20 |
| 3646+1404 | 152 ± 3 | 206 ± 4 | 12 36 46.33 ± 0.02 | 62 14 04.7 ± 0.2 | <2 | 0.960 | 21 |
| 3649+1313 | 22 ± 2 | 22 ± 2 | 12 36 49.61 ± 0.10 | 62 13 13.8 ± 0.6 | <5 | 0.475 | 21 |
| 3651+1221 | 18 ± 3 | 20 ± 3 | 12 36 51.67 ± 0.06 | 62 12 21.1 ± 0.4 | <2 | 0.299 | 24 |
| 3655+1311 | 12 ± 3 | 14 ± 3 | 12 36 55.47 ± 0.11 | 62 13 11.7 ± 0.6 | <3 | ··· | 23 |

[a] Right ascension is given in hours, minutes, and seconds, and declination is given in degrees, arcminutes, and arcseconds.

TABLE 2

Radio Sources in the Hubble Flanking Fields

| Name | Flux Density (μJy) | | Right Ascension[a] (J2000) | Declination[a] (J2000) | Size (arcsec) | $z$ | $I$ |
|---|---|---|---|---|---|---|---|
| | Image | Sky | | | | | |
| 3634+1212 | 40 ± 3 | 90 ± 6 | 12 36 34.46 ± 0.03 | 62 12 12.8 ± 0.2 | <2 | ··· | 19 |
| 3634+1240 | 40 ± 3 | 82 ± 5 | 12 36 34.49 ± 0.03 | 62 12 40.9 ± 0.2 | <2 | 1.215 | 22 |
| 3640+1011 | 30 ± 9 | 324 ± 93 | 12 36 40.68 ± 0.11 | 62 10 11.1 ± 0.6 | 4 | ··· | 25? |
| 3642+1331 | 80 ± 10 | 100 ± 13 | 12 36 42.08 ± 0.02 | 62 13 31.4 ± 0.2 | 3 | ··· | 25 |
| 3646+1448 | 36 ± 13 | 81 ± 30 | 12 36 46.04 ± 0.06 | 62 14 48.7 ± 0.4 | 3 | ··· | >25 |
| 3652+1444 | 121 ± 3 | 256 ± 6 | 12 36 52.88 ± 0.02 | 62 14 44.1 ± 0.2 | <2 | 0.322 | 22 |
| 3653+1139 | 15 ± 3 | 23 ± 5 | 12 36 53.35 ± 0.06 | 62 11 39.7 ± 0.4 | <2 | ··· | 23 |
| 3701+1147 | 19 ± 2 | 41 ± 4 | 12 37 01.59 ± 0.12 | 62 11 47.2 ± 0.5 | <4 | ··· | 24? |
| 3708+1055 | 13 ± 3 | 146 ± 31 | 12 37 08.24 ± 0.10 | 62 10 55.8 ± 0.5 | <3 | ··· | 21 |
| 3708+1245 | 15 ± 2 | 49 ± 8 | 12 37 08.70 ± 0.08 | 62 12 45.0 ± 0.6 | <3 | ··· | 24? |
| 3721+1129 | 100 ± 3 | [b] | 12 37 21.25 ± 0.02 | 62 11 29.7 ± 0.2 | <2 | ··· | 23 |
| 3725+1128 | 48 ± 13 | [b] | 12 37 25.96 ± 0.05 | 62 11 28.3 ± 0.2 | 3 | ··· | 23 |

[a] Right ascension is given in hours, minutes, and seconds, and declination is given in degrees, arcminutes, and arcseconds.
[b] Outside primary beam. Correction factor to the sky flux density from the image flux density is uncertain but greater than 20.

(HFF 3721+1129) may be associated with a ring-shaped galaxy.

## 4. DISCUSSION AND CONCLUSIONS

The first radio image covering the HDF+HFF shows that most of the identifications are with galaxies in the magnitude range 20–24 mag. It is interesting that all of the sources in the HDF above our flux density limit of 12 μJy are identified with galaxies substantially brighter than the HDF detection limit of 29 mag. The most common types are red elliptical galaxies and blue early-type spirals, in agreement with the results from other deep surveys. Many of the identified sources appear to be in groups where interacting galaxies are suspected from the optical and radio morphologies. One radio source at most (less than 5% of the sample) may be in an empty optical field.

For the seven sources with measured redshifts, the monochromatic radio luminosity at 8 GHz is $10^{21}$–$10^{25}$ W $\mathrm{Hz}^{-1}$, comparable to that of nearby Fanaroff-Riley I (FR I) radio galaxies identified with strong radio sources.

Twelve radio sources lie in the flanking fields where the limiting magnitude is about $I = 25$ mag. Eight sources are reliably identified, three have uncertain identifications, and one appears to be an empty optical field. As with the HDF, identifications are associated with elliptical galaxies and early-type spiral galaxies, and many identified sources appear to be interacting with a nearby galaxy, or to be in small groups. The average magnitude of the flanking field identifications is about 23 mag.

The three uncertain identifications in the flanking fields (HFF 3640+1011, HFF 13701+1147, HFF 3708+1245) are displaced more than 1″ from the radio position. Their status should be resolved with better radio-optical astrometry. The empty field containing source HFF 3646+1448 is one of the few slightly extended radio sources. No optical object above 25 mag is seen in the flanking field at the position of the peak of the radio source or within 2″ of it.

Further observations with the VLA have reduced the rms sensitivity from 2.8 to ∼2.1 μJy (Richards et al. 1996). Planned observations with the VLA in the A configuration and with MERLIN (Muxlow T. 1996, private communication) will give a resolution comparable to that of *HST*. In addition, radio spectral information on the ≈30 brightest sources will be obtained with 2″ resolution data at 1.4 GHz. These radio studies, and additional optical work, should further our understanding of both star formation at high redshift and the distinction between radio-loud and radio-quiet early-type spiral galaxies.

This work was made possible through the foresight of R. Williams and the staff of the Space Telescope Science Institute in obtaining and making available the HDF images. We thank David Hogg, who provided the redshifts of galaxies in the HDF, and C. Steidel for providing his astrometric Palomar image. Part of this work was supported by NASA through grant AR-06337.02-94A from the Space Telescope Science Institute, which is operated by the Association of Universities for Research in Astronomy, Inc., under NASA contract NAS5-2655 and by a National Science Foundation grant AST-9320049 to Haverford College. E. A. R. acknowledges the support of a Sigma Xi grant-in-aid-of-research. The National Radio Astronomy Observatory is a facility of the National Science Foundation, which is operated by Associated Universities, Inc., under a cooperative agreement with the National Science Foundation.

## REFERENCES

Cohen, J. G., Cowie, L. L., Hogg, D. W., Songaila, A., Blandford, R., Hu, E. M., & Shopbell, P. 1996, ApJ, submitted
Fomalont, E. B., Partridge, R. B., Lowenthal, J. D., & Windhorst, R. A. 1993, ApJ, 404, 8
Fomalont, E. B., Windhorst, R. A., Kristian, J. A., & Kellermann, K. I. 1991, AJ, 102, 1258
Hammer, F., Crampton, D., Lilly, S. J., LeFevre, O., & Kenet, T. 1995, MNRAS, 276, 1085
Kellermann, K. I., Fomalont, E. B., Richards, E. A., Partridge, R. B., & Windhorst, R. A. 1996, in preparation
Richards, E. A., Fomalont, E. B., Kellermann, K. I., Partridge, R. B., & Windhorst, R. A. 1996, in preparation
Williams, R. E., et al. 1996, AJ, 112, 1325
Windhorst, R. A., Dressler, A., & Koo, D. C. 1987, in IAU Symp. 124, Observational Cosmology, ed. A. Hewitt, G. Burbidge, & L. Z. Fang (Dordrecht: Reidel), 573
Windhorst, R. A., Fomalont, E. B., Kellermann, K. I., Partridge, R. B., Richards, E., Franklin, B. E., Pascarelle, S. M., & Griffiths, R. E. 1995, Nature, 375, 471
Windhorst, R. A., Fomalont, E. B., Partridge, R. B., & Lowenthal, J. D. 1993, ApJ, 405, 498

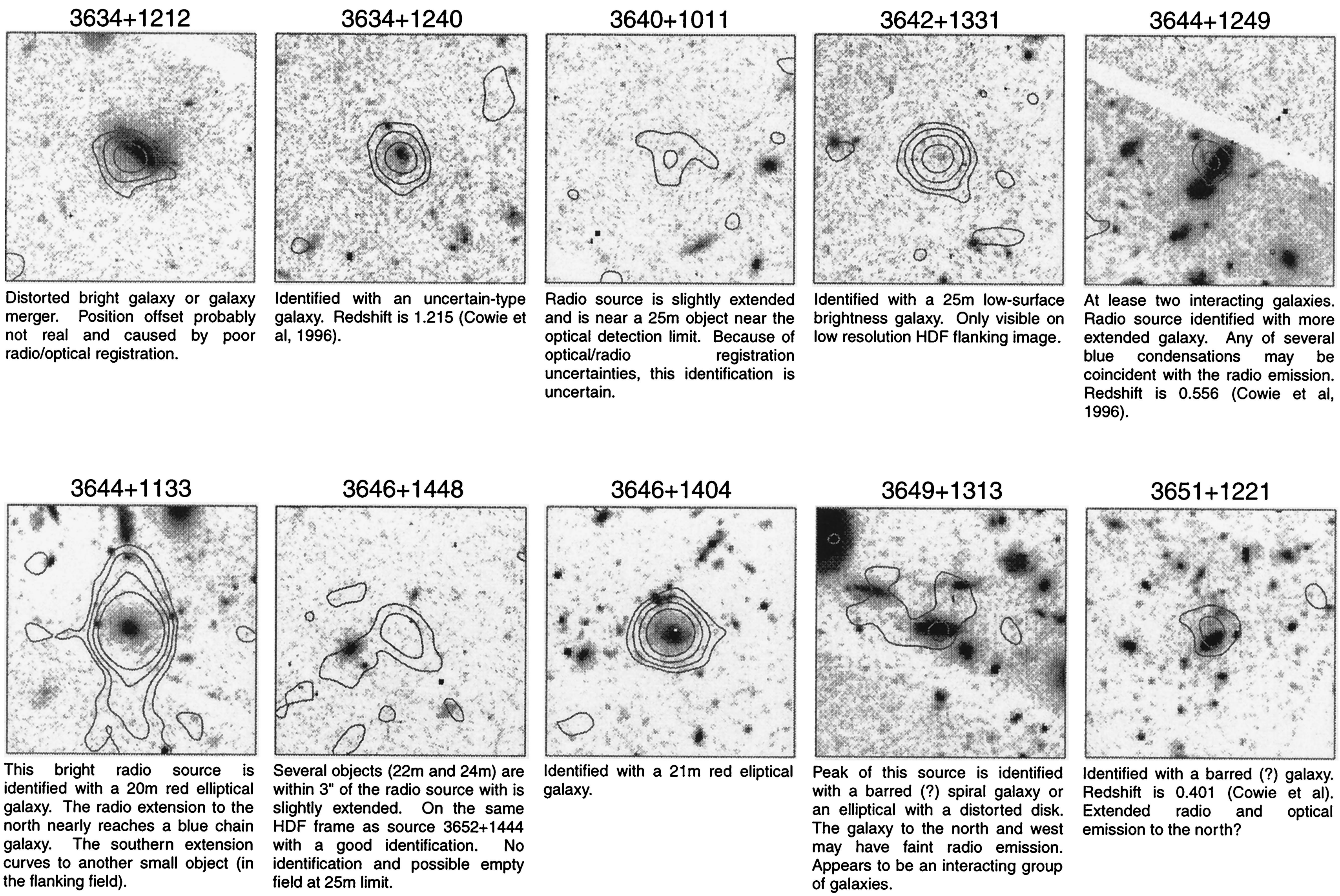


FIG. 2*a*

FIG. 2.—Identification of the 18 sources in the radio image. The gray scale shows the optical emission, and the contours show the radio emission. The contour levels are 6, 12, 18, and 36 $\mu$Jy beam$^{-1}$.

3652+1444

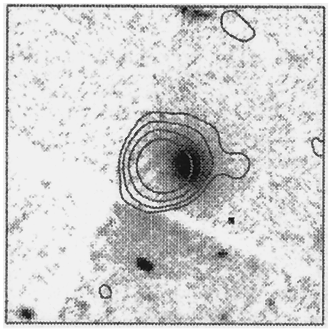

Identified with 22m red elliptical galaxy. Position offset probably caused by registration error.

3653+1139

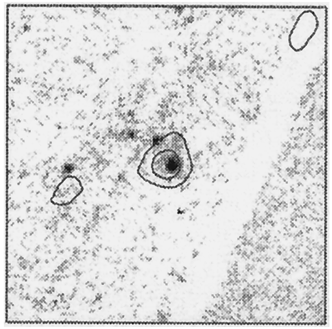

Identified with a 23m galaxy.

3655+1311

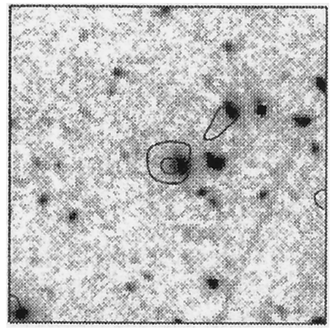

Identified with a 23m red elliptical galaxy.

3655+1340

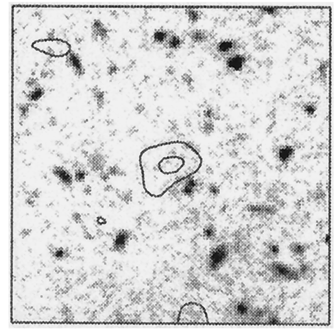

A 23.5m double-galaxy is 2" south of radio source. Nothing at HDF limit at radio peak. Good radio optical registration on this frame. Source unidentified.

3701+1147

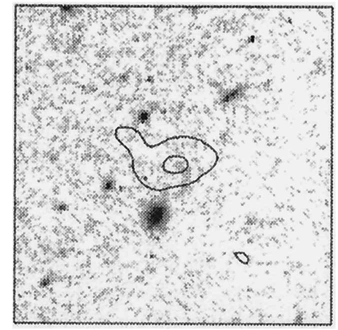

Radio centroid about 3" from 22m galaxy. A faint arc of optical emission may be associated with the source.

3708+1055

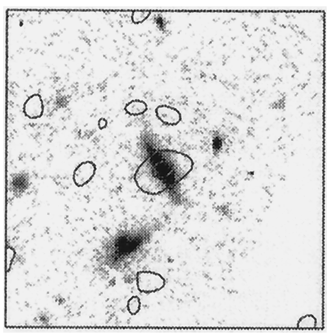

Identified with a 21m spiral galaxy.

3708+1245

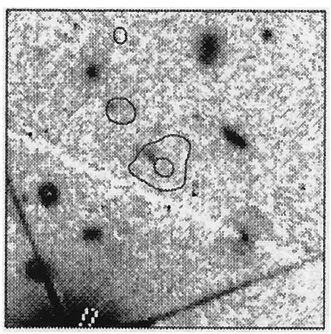

Within 0.5" of 24m galaxy. Looks distorted and may be interacting pair.

3721+1129

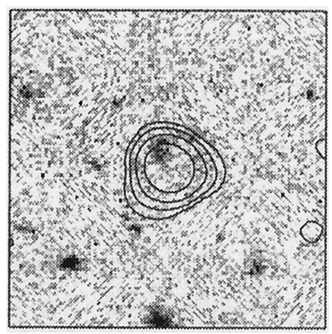

Identified with a 23m ring (?) galaxy. Flux density of source is uncertain, but > 3mJy.

3775+1128

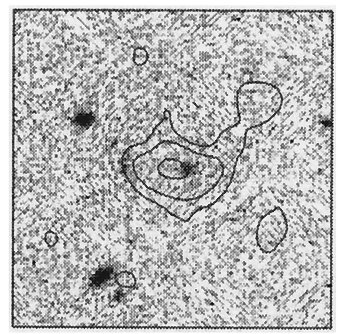

Radio source is slightly extended. Identified with a 23m galaxy with an extended (?) nucleus. Flux density of source is uncertain, but > 1.5mJy.

FIG. 2*b*